Journal of Research in Nondestructive Evaluation

ISSN: 0934-9847 (Print) 1432-2110 (Online) Journal homepage: https://www.tandfonline.com/loi/urnd20

Determination of All Elastic Constants of Orthotropic Plate Specimens from Group Velocity Data

K. Y. Kim , T. Ohtani , A. R. Baker & W. Sachse

To cite this article: K. Y. Kim , T. Ohtani , A. R. Baker & W. Sachse (1995) Determination of All Elastic Constants of Orthotropic Plate Specimens from Group Velocity Data, Journal of Research in Nondestructive Evaluation, 7:1, 13-29, DOI: 10.1080/09349849509409563

To link to this article: https://doi.org/10.1080/09349849509409563

Published online: 21 Apr 2009.

Res Nondestr Eval (1995) 7:13–29

Determination of All Elastic Constants of Orthotropic Plate Specimens from Group Velocity Data

K.Y. Kim[1], T. Ohtani[2], A.R. Baker[1], and W. Sachse[1]

[1]Department of Theoretical and Applied Mechanics, Thurston Hall, Cornell University, Ithaca, New York 14853; [2]Ebara Research Corporation, Materials Laboratory, 4-2-1 Hon-Fujisawa, Fujisawa, Kanagawa 251, Japan

Abstract. This paper presents a novel method of nondestructively determining all nine elastic constants of fiber-reinforced orthotropic plate specimens. Group velocities of bulk quasi-longitudinal (QL), pure transverse (PT), and surface skimming pseudo-longitudinal modes are measured in glass-fiber (GF) and carbon-fiber (CF) reinforced Poly Ether Ether Ketone (PEEK) specimens by a point-source/point-receiver (PS/PR) technique. First, the pure index longitudinal moduli C_{11}, C_{22}, and C_{33}, are obtained from the longitudinal (L) group velocities measured in three principal directions. Next, the pure index shear moduli, C_{44}, C_{55}, and C_{66}, are determined by measuring the shear horizontally (SH) polarized PT group velocities in the symmetry planes. Finally, the mixed index elastic constants C_{ij} $(i \neq j)$ are calculated from QL group velocities measured in the symmetry planes and using analytic formulas.

Introduction

Analytic relations between the elastic constants of elastically anisotropic media and the acoustic phase velocities propagating in a general direction in the media are conveniently found in the solution of Christoffel's equation [1–3]. In an anisotropic medium, the phase and group velocities do not coincide in a general direction of propagation. No closed-form analytic formula can easily be found between a group velocity and elastic constants for an arbitrary propagation direction in an anisotropic medium. Consequently, the elastic constants are most often determined using the measured phase velocity data. The measurement methods are excellently reviewed in the literature [4–6]. The phase velocities are usually measured along the symmetry directions because the measurement errors along these directions are minimal, and there exist relatively simple explicit relations between the phase velocities along these directions and the elastic constants.

In the symmetry directions of materials, the phase and group velocities coincide with each other and this provides valuable relations between the elastic constants and the group velocities. While the measurements of either phase

or group velocities along the symmetry axes using both longitudinal (L) and transverse (T) modes are sufficient to obtain all three elastic constants of a cubic medium, additional measurements are required in a nonsymmetry direction to determine all the elastic constants for media with transversely isotropic or lower symmetry. Recently, Rokhlin and Wang [7] described a double through-transmission technique by which all elastic constants of media with orthorhombic or higher symmetry can be obtained from the measured bulk wave phase velocities. More recently, closed-form analytic formulas have been developed that relate the elastic constants of media with orthorhombic or higher symmetry to the group velocities measured along arbitrary directions in the principal symmetry planes [8].

In this work all nine elastic constants associated with orthotropic fiber-reinforced poly ether ether ketone (PEEK) plates are determined, using the measured group velocities along the various directions in the symmetry planes and the formulas from Ref. 8. The group velocities in various directions are measured by using pointlike sources and pointlike detectors and changing their relative orientation. The pointlike sources include a fracture of a tiny glass capillary and small shear (S) mode piezoelectric PZT transducer. The pointlike detectors employed are small PZT transducers of L or S mode sensitivity.

Theoretical Backgrounds

Analytic Relations between Elastic Constants and Group Velocity in Symmetry Planes

Consider a medium with orthotropic symmetry for which three principal axes of symmetry are denoted by x_1, x_2, and x_3 directions. For waves traveling in the three symmetry planes, i.e., x_1x_2, x_2x_3, and x_1x_3 planes, once the relation between the elastic constants and sound wave speed is found for one of these planes, similar relations can be obtained for the other two planes by the proper rotation of indices. Therefore, we consider a wave traveling, for example, in the x_1x_3 plane with its wave normal $\mathbf{n}$ and group velocity $\mathbf{V}_g$ oriented at angles θ and ζ, respectively, to the x_3 axis, as depicted in Fig. 1. The positive sense of both θ and ζ is taken in a clockwise direction from the x_3 axis. Because of the

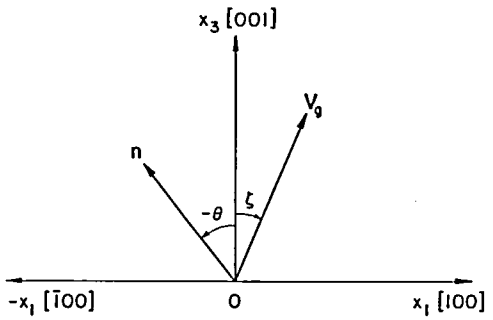

Fig. 1. Coordinate systems for group and phase velocities.

reflection symmetry of the x_1x_3 plane across the x_1 axis for media of orthotropic or higher symmetry, we restrict, without loss of generality, the range of both ζ and θ between $-90°$ and $90°$, that is, $-90° \leq \zeta, \theta \leq 90°$. The orthotropic medium is characterized with nine elastic constants: C_{11}, C_{22}, C_{33}, C_{44}, C_{55}, C_{66}, C_{12}, C_{13}, and C_{23}.

Because of mirror symmetry across the symmetry planes, all the points in the symmetry plane of the normal or slowness surface will map themselves on the corresponding symmetry plane in the group velocity or ray surface. However, except for a transversely isotropic medium, the converse is not in general true, as is well known in the theory of phonon focusing [9, 10]. Since the shape of the quasi-transverse (QT) mode slowness surface of an anisotropic medium is nonspherical, concave or convex, some points with their wave normals that do not lie in the symmetry plane of the QT slowness surface may map themselves onto the symmetry plane of the group velocity surface. The group velocity sections that do not correspond to the symmetry plane of the normal or slowness surface are not of interest here and we deal only with those group velocity sections that correspond to the symmetry planes of the slowness surfaces.

Formulas relating phase velocity to the elastic constants of solid media are described by many authors [1–3]. For waves traveling in the principal symmetry directions, the phase and group velocities of both L and T modes coincide with each other and simple relations exist between the elastic constants and the wave speed. The L waves traveling with speed V_L along the x_1, x_2, and x_3 directions yield, respectively,

$$\rho V_L^2 = C_{11}; \quad \rho V_L^2 = C_{22}; \quad \rho V_L^2 = C_{33}. \tag{1}$$

The pure index shear moduli can be calculated from the T modes propagating in the principal axis directions. One obtains from the transverse waves propagating with speed V_T along the x_3 direction and polarized in x_1, and x_2 directions, respectively.

$$\rho V_T^2 = C_{55}; \quad \rho V_T^2 = C_{44}. \tag{2}$$

Similarly, C_{44}, C_{55}, and C_{66} can be determined from the speeds of pure transverse waves propagating in the x_1 and x_2 directions. Equations (1) and (2) indicate that all pure index elastic moduli can be obtained from the pure L and T waves traveling along the principal symmetry directions of a medium. The pure index shear moduli can also be determined from the pure transverse (PT) modes propagating in an arbitrary direction of the symmetry planes. A simple formula that relates a group velocity to ζ is found for the PT waves with shear horizontal (SH) polarization [1, 2] and is given by

$$\frac{1}{\rho V_g^2} = \frac{\sin^2 \zeta}{C_{66}} + \frac{\cos^2 \zeta}{C_{44}}. \quad \text{(PT mode)} \tag{3}$$

Equation (3) indicates that two shear elastic moduli, C_{44} and C_{66}, can be obtained by measuring the group velocities of PT modes propagating in at least

two different directions. By performing similar measurements in the x_1x_2 and x_2x_3 planes, all the shear moduli, C_{44}, C_{55}, and C_{66}, can be obtained.

One the pure index elastic moduli, C_{11}, C_{22}, C_{33}, C_{44}, C_{55}, and C_{66}, are determined by the method described above, the mixed index elastic moduli, C_{12}, C_{23}, and C_{13}, can be obtained from the group velocity measurement of either quasi-longitudinal (QL) or QT mode propagating along an arbitrary direction in the x_1x_2, x_2x_3, and x_1x_3 planes, respectively. Again we take the case of a wave traveling in the x_1x_3 plane. Explicit analytic expressions for the group velocities of QL and QT modes as a function of a general direction in the symmetry plane are given in Ref. 8 and these formulas are applicable to the symmetry planes of solid media with orthotropic or higher symmetry.

We define for simplicity of notation the following identities:

$$C_{11\pm} \equiv C_{11} \pm C_{55}, \tag{4}$$

$$C_{33\pm} \equiv C_{33} \pm C_{55}, \tag{5}$$

$$C_{13\pm} \equiv C_{13} \pm C_{55}. \tag{6}$$

$$B \equiv C_{11-}C_{33-} - 2\,C_{13+}^2, \tag{7}$$

$$p \equiv \tan\theta, \qquad q \equiv \tan\zeta, \tag{8}$$

$$D \equiv [(C_{11-}p^2 - C_{33-})^2 + 4C_{13+}^2p^2]^{1/2} > 0. \tag{9}$$

It can be then shown that B in Eq. (7) and the above D are related by

$$B = \frac{1}{2p^2}(C_{11-}^2p^4 + C_{33-}^2 - D^2). \tag{10}$$

Kim [8] has derived the following Eqs. (11)–(15). The relationship between the directions of group velocity and wave normal is given by

$$q = p\,\frac{B - C_{11-}^2p^2 \mp C_{11+}D}{Bp^2 - C_{33-}^2 \mp C_{33+}D}, \tag{11}$$

which with the substitution of Eq. (10), yields

$$q = \frac{D^2 \pm 2C_{11+}Dp^2 + C_{11-}^2p^4 - C_{33-}^2}{p(D^2 \pm 2C_{33+}D - C_{11-}^2p^4 + C_{33-}^2)}. \tag{12}$$

We express Eq. (11) in the form of

$$C_{11-}^2p^3 + q(Bp^2 - C_{33-}^2) - Bp \pm (C_{11+}p - C_{33+}q)\,D = 0. \tag{13}$$

Equation (11) or (13) can be used to find the wave normal corresponding to a given group velocity direction lying in the same corresponding symmetry plane and vice versa. Equation (12) is quadratic in D, the solution of which as a function of $p = \tan\theta$ can be written as

$$D(p) = \frac{1}{1 - pq}\{p(\pm C_{33+}q \mp C_{11+}p) \pm [p^2(C_{33+}q - C_{11+}p)^2 - (1 - p^2q^2)(C_{11-}^2p^4 - C_{33-}^2)]^{1/2}\}. \tag{14}$$

In the above equation, we choose the region of $p = \tan\theta$ where D is real and positive. Finally, the relation for group velocity is given by

$$\rho V_g^2 = \frac{(1 + q^2)(C_{11-}^2p^4 - C_{33-}^2 \mp 2C_{33+}D - D^2)^2}{8D^2(C_{11+}p^2 + C_{33+} \pm D)}. \tag{15}$$

The upper and lower signs either in $\pm$ or in $\mp$ in Eqs. (11)–(15) apply to the QL and QT modes, respectively, except in the $\pm$ sign in front of the square bracket for square root in Eq. (14), which applies to both QL and QT modes.

Equation (15) expresses the group velocity as a function of $p = \tan\theta$, when D is replaced by the expression on the right hand side of Eq. (14). Usually, experimentally or by other means as described in this section, the magnitude of group velocity V_g, its direction ζ, C_{11+}, C_{11-}, C_{33+}, and C_{33-}, are known. Then, Eq. (15) can be solved to find $p = \tan\theta$, which makes D in Eq. (14) real and positive. Once this value of $p = \tan\theta$ is found, one can obtain the values of D, B, C_{13+}, and finally C_{13} by using Eqs. (14), (10), (7), and (6), respectively. On the other hand, if the known values of all elastic constants of a medium are given, Eq. (11) or (13) can be combined with Eq. (15) to predict the value of QL or QT group velocity in any direction in the symmetry plane.

Now we consider an elastic wave propagating in the x_2x_3 plane, having group velocity $\mathbf{V}_g$ and its wave normal $\mathbf{n}$ at angles ζ and θ to the x_3 axis, respectively. In this case, we replace the subscript index number 1 in the notations of the elastic constant C_{ij}, by the subscript index 2 and C_{55} by C_{44} in all the appropriate equations following Eq. (3). With these replacements, Eqs. (14) and (15) can be applied to find the root $p = \tan\theta$ and the corresponding value of D for the QL and for the QT modes. Once the value of D is known, the mixed index elastic constant C_{23} can be obtained by using the relations corresponding to Eqs. (10), (7), and (6) for each mode.

Finally, we consider an elastic pulse propagating in the x_1x_2 plane with $\mathbf{V}_g$ and $\mathbf{n}$ at angles ζ and θ to the x_1 axis, respectively. We first replace C_{55} by C_{66} and substitute the subscript index 3 by 1 and the subscript index 1 by 2 in the notations of the elastic constants C_{ij} in all the appropriate equations following Eq. (3). With these replacements, the elastic constant C_{12} can be obtained in a similar way as described for the QL and QT mode propagations in the x_2x_3 or x_1x_3 plane.

For extension of Eqs. (11)–(15) to higher symmetry groups and the face-diagonal planes of tetragonal and cubic media, readers should refer to Ref. 8.

On Identification of the Arrival of a SH Polarized PT Mode

The accuracy of the elastic constants determined by wavespeed measurements is directly related to the ability to determine the arrival time of various modes. The QL group velocity can be easily and accurately measured, since its arrival

in the detected signal is unambiguously identified as the point from which the signal first exceeds the noise level. Materials in which the transverse group velocity exceeds the QL group velocity are extremely rare and will not be considered further. However, the PT wave arrival, being slower than the QL mode, is not always easy to identify. The determination of C_{44} and C_{66} from the group velocities of the SH polarized PT modes via Eq. (3) and similarly the determination of C_{55} and C_{66} from the SH polarized PT waves propagating in the x_2x_3 plane require a clear identification of the arrival of the PT mode. In the next section, the SH polarized group velocities have been measured at several points on a specimen surface belonging to the x_1x_3 or x_2x_3 symmetry plane. A PZT shear source and a PZT shear detector are used. Both are polarized in the same direction normal to the symmetry plane. The SH motions can be caused by the arrival of all three modes, i.e., QL, QT, and PT modes. The identification of the SH motions corresponding to the QL, QT, and PT modes in the detected signal depends mainly on the following factors: first, the type of detected used; second, whether the detector is situated in the near or far field of the source; and third, whether the detector is in a direction within or outside a cuspidal region of the QT mode. For an isotropic solid, the transverse sheet is spherical and there is no cusp in any direction. However, for an anisotropic solid, depending on the shape of its slowness surface, there can be one or more foldings in some directions, or no cusp in any direction [10, 11]. In the cuspidal region belonging to the symmetry plane, the QT group velocity sheet is folded and in addition the the QL and PT group velocity branches, there are three group velocity branches of the QT sheet that are mapped from the wave normals in the corresponding symmetry plane of slowness: fast QT (FQT), intermediate speed QT (IQT), and slow QT (SQT) branches. Outside the cuspidal region in the symmetry plane, there is one QT branch in addition to one QL and one PT branches.

The S PZT source located on the surface of a specimen when its polarization is aligned along the x_1 direction parallel to the [100] can be modeled as a monopolar source acting in the [100] direction. Any direction on the top or bottom surface plane (001) is identical to the [100] in a (transversely) isotropic material. With a Heaviside step source acting at origin, the SH polarized transverse displacement response, $\tilde{G}_{11}(\mathbf{x}, t)$, as a function of the detector position $\mathbf{x}$ and time t, is described by Every and Kim [12]. Inside a cuspidal region, the $\tilde{G}_{11}(\mathbf{x}, t)$ shows a barely perceptible kink (change in slope) at the QL arrival, a sharp kink at the FQT arrival, a discontinuity at the PT arrival, a moderate kink at the IQT arrival, and a sharp kink at the SQT arrival. Outside the cuspidal region, the arrival of the QL mode causes a barely noticeable kink, followed by a discontinuity at the PT mode arrival. The thin disk-shaped PZT detected used in our experiment is observed to be principally sensitive to the changing slope of a temporal displacement signal. The change in slope is large at the sharp kink and the largest at the discontinuity caused by the PT arrival, and hardly noticeable at the QL arrival. Further, the SH motions caused by the arrival of the QL mode is a near-field effect, diminishing with the inverse square of the distance r from a source to a detector. Consequently, it is difficult to observe in a far-field. Because of thin specimens (about 3 mm thickness), the distance r in our experi-

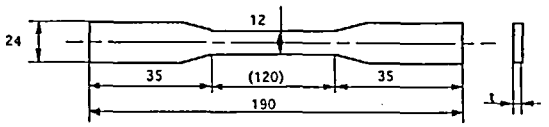

Fig. 2. Geometry and dimension of PEEK specimens in mm.

ment lies in the near field. Indeed, we observe that the S PZT detector used in our experiment detects the SH motions caused by the arrivals of QL, QT, and PT models. The SH motion at the arrival of the QL mode is so weak in amplitude that it is buried under the noise and cannot be detected, even though the subsequent SH motions following the QL arrival are detectable with a little difficulty. It is quite difficult to identify the arrival of single or various QT modes outside and within the cuspidal region in the signal detected by a thin-disk shaped PZT transducer, but this difficulty is not of importance for the identification of the PT mode arrival. Fortunately, these effects are much less pronounced in the SH motions following the PT mode arrival because its arrival causes a large swing in amplitude, overwhelming the effects of other modes and making its identification easy

Experimental Setup

Three different kinds of poly ether ether ketone (PEEK) specimens were provided by the Mitsui-Touatsu Chemical Company, Japan: natural (no fiber imbedded) PEEK (NT PEEK), glass-fiber reinforced PEEK (GF PEEK), and carbon-fiber reinforced PEEK (CF PEEK). The geometry and dimensions of the PEEK specimens are displayed in Fig. 2, and their material properties are listed in Table 1.

The transducer locations used in all the measurements are shown in Fig. 3. The source, either a capillary fracture or a line-type S PZT, is always activated on the top surface at the widest part of the specimen. The detector, an L or S mode 0.75 mm diameter PZT transducer, is positioned on the bottom surface for all measurements, except for detecting the surface skimming L mode.

The line-type S PZT source consists of a narrow rectangular-shaped element, 5 mm long, 0.75 mm wide, and polarized in the 5 mm direction. It is positioned at locations along the x_1 and x_2 axis to measure the PT group veloci-

Table 1. Specimen specifications.

Specimen	Density (kg/m^3)	Fiber Weight Fraction	Thickness (mm)
Natural (NT)	1300		3.12
Glass Fiber (GF)	1400	20%	3.06
Carbon Fiber (CF)	1440	30%	3.26

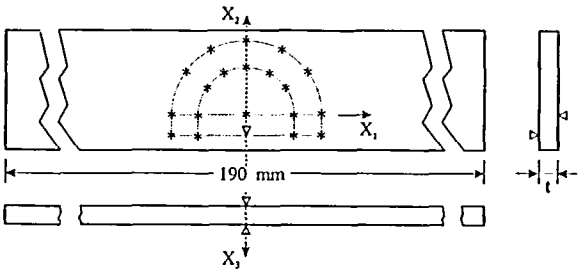

Fig. 3. Geometric schematic of capillary fracture and S PZT sources with L or S PZT detector.

ties. The choice of the line-type S PZT source, in lieu of a pointlike S PZT source for measurement of PT group velocity, is simply a matter of convenience in identifying the PT mode arrival by enhancing the ratio of the SH motion associated with the PT arrival to that associated with the arrivals of other modes polarized in the sagittal plane. A high voltage pulse from a Panametrics Model 5055PR is used to excite the transducer. Elastic waves generated by the S PZT source propagate to the opposite face of the specimen, where they are detected by the pointlike S PZT transducer. The arrival times of the SH polarized PT mode is actually determined in the following way. As mentioned in the previous section, the first large amplitude in the detected signal is found at the arrival of the PT mode following that of the QL mode. The maximum amplitude in the signal occurs when the polarization of the detector is aligned parallel to that of the source, the polarization of which is normal to the symmetry plane. As the detector rotates, the portion of the signal corresponding to the PT mode is dramatically reduced in amplitude. The beginning of this portion of the waveform is taken as the PT mode arrival. A waveform recorded with the CF PEEK specimen is displayed in Fig. 4, where PT indicates its arrival time. The method of measuring the PT mode group velocity in a thick plate-shaped specimen by using the point source (PS) and point detector (PD) has been previously described in the papers of Kim et al. [13, 14].

For the QL and L wave measurements a capillary fracture source and a pointlike L PZT detector are used. A 0.08 mm thick polyvinylidene fluoride (PVDF) film is laid (refer to Fig. 5) on the top surface of the specimen and a glass capillary of diameter less than 0.1 mm is broken on the PVDF film by slowly pressing the capillary with a sharp razor blade. The capillary fracture source has a vertical force drop with Heaviside step time dependence [15]. The force is measured via a miniature load cell attached to the razor blade and ranges typically from 5 to 10 N. Broadband signals generated by the capillary fracture source propagate through the specimen and are detected by the L PZT transducer. The arrival of L mode in the detected signal is unambiguously identified as the first point from which the signals exceeds a noise level as aforementioned. The arrival times of the L mode are used to calculate the QL group velocities in various directions.

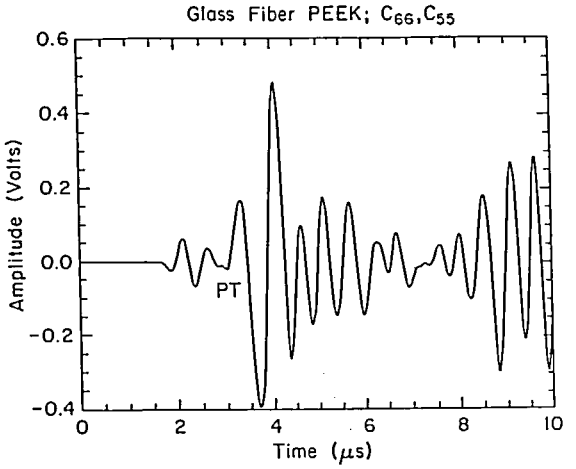

Fig. 4. A typical off-epicentral SH signal detected by the S PZT transducer located in the x_2x_3 plane with a line-type S PZT source. Both source and detector are polarized in the x_1 direction.

The detected signals are amplified with 40 or 60 db gain by a low noise preamplifier, the bandwidth of which extends from 20 kHz to 2 MHz. The amplified output is fed into a digitizer (Tektronix AD 390), where it is sampled at a 60 MHz sampling rate with a 10-bit resolution, and the digitized signal is displayed on an x-y scope for visual observation. The output of the PVDF film generated at the instant of capillary fracture serves as a trigger to the digitizer

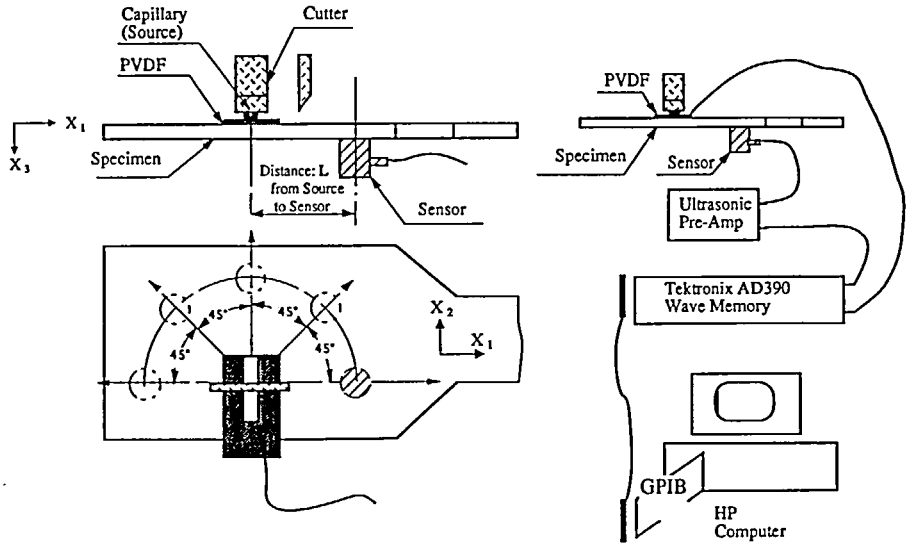

Fig. 5. Electronic block diagram of the experimental set-up with capillary fracture source and L PZT detector on the top and bottom surfaces, respectively.

and also indicates the time of source excitation that provides a time of reference for measurements of travel times of various rays propagating from the source to the detector. All these data are stored on the hard disk of a microcomputer for subsequent signal processing and analysis. The electronic block diagram with a capillary fracture source and an L PZT detector on the bottom face is shown in Fig. 5.

Determination of Elastic Constants

Identification of Anisotropy

The three obtained PEEK specimens are assumed to be elastically anisotropic, and their anisotropic types and the directions of principal axes are presumed to be unknown. To determine the anisotropy and principal axes of the materials and also the wavespeeds of various modes, a series of experiments is performed in which various configurations of the source and detector are used.

First, the glass capillaries are broken on the 0.08 mm thick PVDF film laid on the top surface of the specimen at positions forming a semicircle of 15 mm radius. The L mode PZT detector is located at the center of the semicircle on the top surface. The first arrival of the signal is associated with a surface skimming pseudo-longitudinal wave that propagates at the same speed as the corresponding bulk L wave. Figure 6 shows a measured pseudo-L mode group velocity pattern, which indicates two-fold symmetry across the x_1 and x_2 directions for the GF and CF PEEK materials, with the maximum and minimum L speeds along the x_1 and x_2 directions, respectively, and transverse isotropy in the x_1x_2 plane for the NT PEEK material. The pattern suggests that the x_1 and x_2 directions may be the two principal axes, while for the NT PEEK it suggests transverse isotropy about the x_3 axis.

Second, using the same source configuration as in the first case except with the L mode detector situated on the bottom face of the specimen at the center of the 5 mm radius semicircle, the QL group velocities are measured and plotted in Fig. 7. The group velocity profile in the figure supports the premise made above that the NT PEEK is transversely isotropic in the x_1x_2 plane. The group velocity patterns of CF and GF PEEKs exhibit a mirror symmetry across the x_1x_2 and x_2x_3 planes and also indicate the maximum and minimum L group velocities on these two planes, implying that the x_1x_3 and x_2x_3 planes may be the principal symmetry planes and the x_3 direction may be the third principal direction.

Third, with the L mode PZT detector fixed at origin on the bottom face, the capillary fracture sources are scanned across the epicenter along the x_1 and x_2 directions on the top surface. The obtained L group velocity pattern exhibits two-fold symmetry for all three PEEK materials across the x_3 direction along which the group velocity is minimum, indicating that the x_3 direction is indeed one of the principal directions. Furthermore, the L group velocities of the NT peek specimen in the x_3 and other directions are found within experimental error to be equal to those of the surface-skimming pseudo-L wave in the x_1x_2 plane. This indicates that NT PEEK is elastically isotropic. The QL group

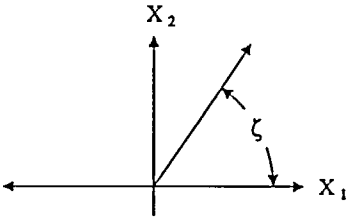

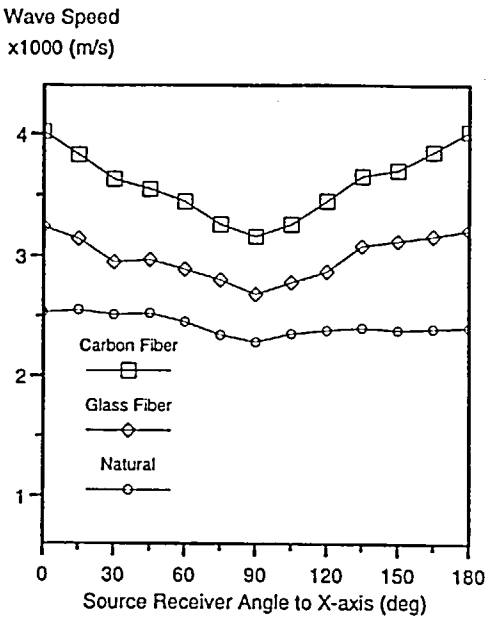

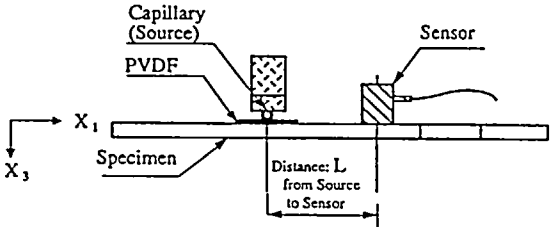

Fig. 6. Directional pattern of pseudo-L wave group velocity on the surface.

velocities in the x_1x_2 plane, obtained by moving the source in the x_1 direction, is displayed in Fig. 8.

Fourth, the same scanning configuration as in the third case above is employed, but the capillary source and L detector are replaced by the line-type S PZT source and pointlike S PZT detector. Both PZT transducers are polarized in the same direction normal to the scanning direction. The observed SH polar-

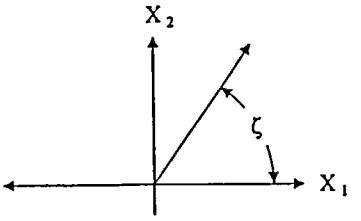

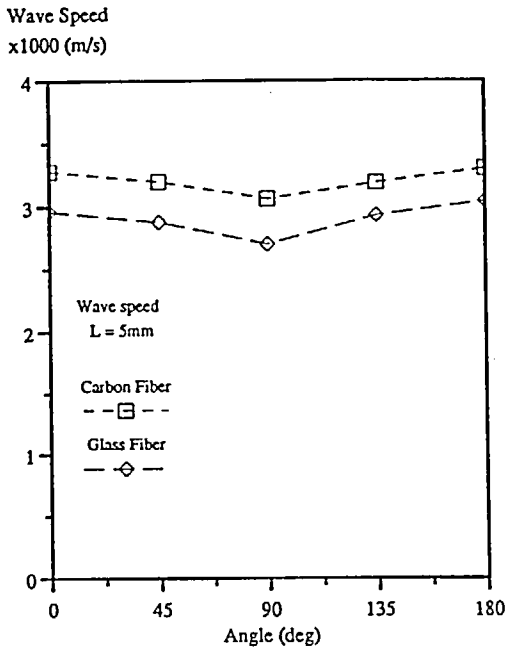

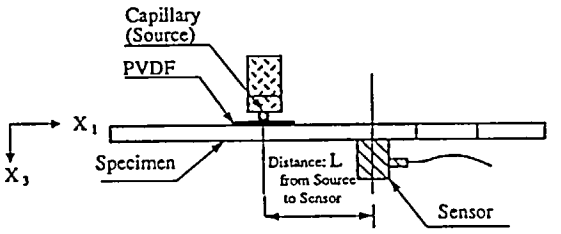

Fig. 7. Directional pattern of bulk QL wave group velocity in the planes of the [001] zone.

ized PT group velocity pattern indicates the same profile as in the third case, with the minimum PT speed along the x_3 direction, thus further supporting the conclusion drawn above with the third configuration. Figure 9 exhibits the group velocities of the PT mode propagated in the x_2x_3 plane.

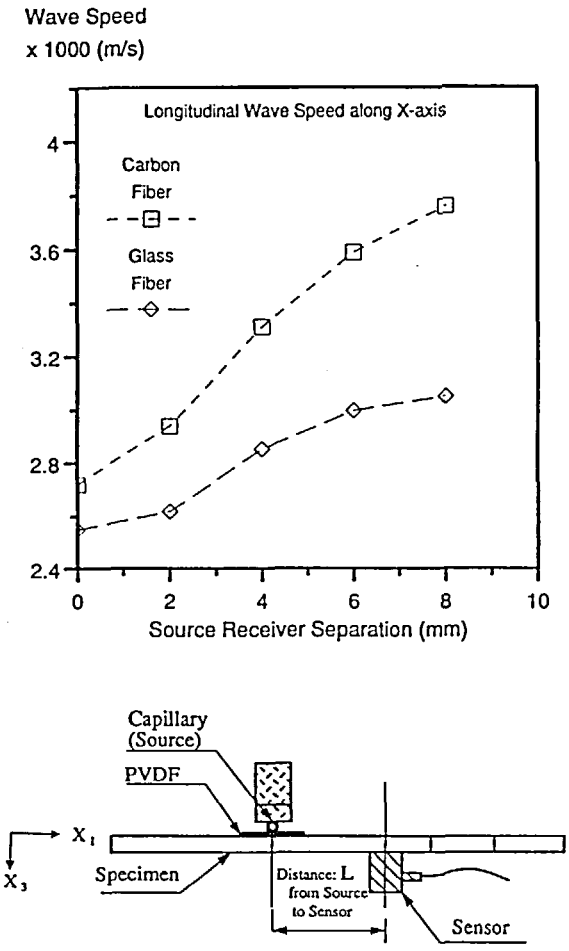

Fig. 8. QL group velocities along various directions in the x_1x_3 plane.

From the above observations, it is concluded that the NT PEEK specimen possesses isotropic symmetry in all directions. The GF and CF PEEK specimens exhibit orthotropic symmetry for which the x_1, x_2, and x_3 directions coincide with the three principal axes. Both materials have minimum longitudinal and transverse wave speeds along the x_3 direction.

Determination of All Elastic Constants

With the anisotropy and principal axes of specimens determined as above, we can now find the two Lame constants of the NT PEEK specimen and all nine elastic constants of the GF and CF PEEK specimens. For the isotropic NT PEEK specimen, $C_{11} = C_{22} = C_{33}$; $C_{44} = C_{55} = C_{66}$; $C_{12} = C_{13} = C_{23}$; $C_{12} = C_{11} - 2C_{44}$; and the two Lame constants λ and μ are given by $\lambda = C_{12}$ and $\mu = C_{44}$.

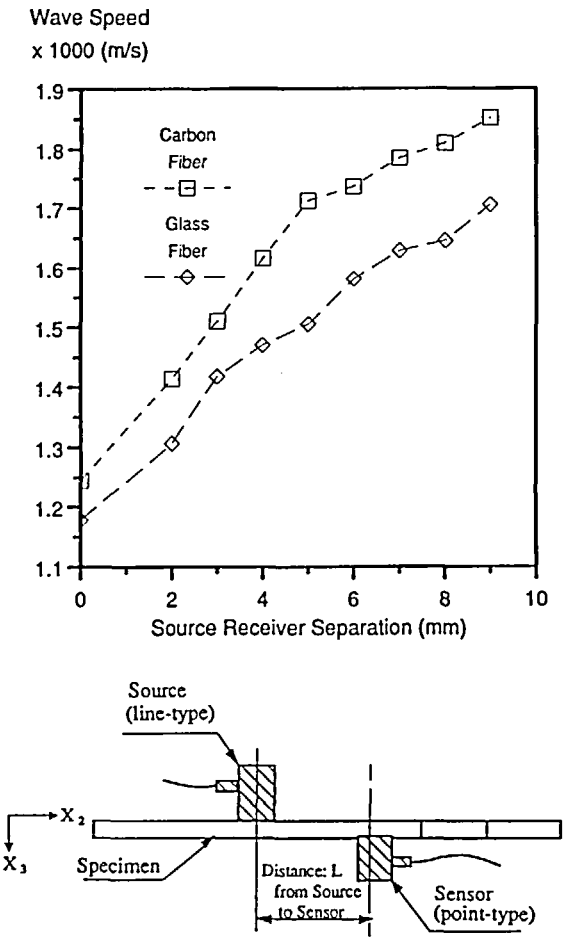

Fig. 9. PT group velocities along various directions in the x_2x_3 plane.

Several L group velocities along the x_3 direction are measured by breaking the glass capillary at many different spots on the top surface and placing the L detector at epicentral positions on the bottom face. Several percent nominal variation in the wavespeeds are observed because of the inhomogeneity of the material. The average value of the squared wavespeeds is used to calculate the elastic constant C_{33}, according to Eq. (1). Similarly, with the L PZT detector at origin on the top surface, C_{11} and C_{22} are obtained from the average of the pseudo-L wavespeeds in the x_1 and x_2 directions, respectively. These L waves are launched from the capillary fracture sources scanned in the x_1 and x_2 directions on the top surface.

Next, the pair of C_{44} and C_{66} values can be determined by fitting the SH polarized PT group velocities obtained in the x_1x_3 plane into the form of Eq. (3). Similarly, the pair of C_{55} and C_{66} values is obtained from the PT group velocities in the x_2x_3 plane. The identification of the arrival times of the SH polarized PT

Table 2. Elastic constants of PEEK specimens in units of GPa.

Specimen	C_{11}	C_{22}	C_{33}	C_{44}	C_{55}	C_{66}	C_{12}	C_{13}	C_{23}
NT PEEK*	7.72			1.49			4.74		
GF PEEK	15.12	10.89	9.36	2.00	2.09	4.26	5.29	6.26	6.46
CF PEEK	28.52	15.21	10.65	2.23	2.41	5.71	7.70	6.00	7.65

* For isotropic NT PEEK: $C_{11} = C_{22} = C_{33}$; $C_{44} = C_{55} = C_{66}$; $C_{12} = C_{13} = C_{23}$; $C_{12} = C_{11} - 2C_{44}$

mode in the detected signals (see, e.g., Fig. 4) has already been described in detail. The average value of several determinations of the elastic constant is taken to represent that of the pure index shear modulus.

The mixed index elastic constants are calculated from the QL group velocity data obtained along arbitrary directions in the principal planes, using Eqs. (14) and (15). The capillary fracture source and L mode PZT detectors are used for this purpose. The average of C_{12} values for the orthotropic PEEK specimens is obtained from the pseudo-L wave group velocity data measured in several different directions with both source and detector located on the top surface. We notice that the longitudinal group velocity through the thickness (x_3-) direction is minimal for the GF and CF PEEK specimens as compared with that of the other principal directions (see Table 2) and the surface skimming pseudo-L wave on the top surface arrives first at the detector, ahead of other plate modes. Since the detector is located near a source (less than 30 mm from it), the first arrival is easily identified. The average C_{13} value is obtained from the QL group velocity data measured along several different directions in the x_1x_3 plane with the source and detector located on the top and bottom sides, respectively. Finally, the averaged C_{23} value is obtained with the source and detector located in the x_2x_3 plane on the opposite sides of the specimen. All the elastic constants of NT, GF, and CF PEEK specimens are compiled in Table 2.

Discussion

The pure index L moduli, such as C_{11}, C_{22}, and C_{33}, are most easily obtained with the least error, from the L group velocities, for their arrival is easily identified in the detected signal. Similarly, the pure index shear moduli, C_{44}, C_{55}, and C_{66}, can also be easily determined for a thick specimen oriented in the principal plane, provided a detector can be located in the far-field of the source. For a relatively thin specimen, the shear moduli can be determined with a little difficulty, as discussed previously. The arrival of the SH polarized PT mode is found by rotating the S PZT source relative to the detector.

The QL and QT modes are coupled in a broadband signal and they are polarized mutually perpendicular to each other in the same sagittal plane. Hence, either the QL or the QT mode can be used for the determination of mixed index elastic constants, C_{12}, C_{23}, and C_{13}, but it is highly recommended to choose the arrival time of the QL mode because of its unambiguous identifi-

cation. Except in a signal detected by a displacement transducer, such as a capacitive transducer, the identification of the QT mode arrival is generally quite difficult in a broadband signal. The problems arising when using thin disk-shaped piezoelectric transducers are: the QL mode lingers on; the detecting transducer rings for a while; and for some directions, a head wave is superimposed on the QT mode. There is another reason why the QL group velocity is preferred—there is no folding of the QL ray surface for which there are no cusps, because the corresponding QL slowness surface is everywhere convex for all media [16]. All the points on the symmetry plane of both the QL and QT slowness surfaces map into the corresponding symmetry plane of group velocity surfaces. However, the converse is not true for the QT mode of anisotropic media with symmetry lower than transverse isotropy. Depending on the direction, the QT slowness surface is concave, convex, or transitional between them. Some points of zero Gaussian curvature which lie outside the symmetry planes of the QT slowness surface may have their caustics mapped across the mirror symmetry plane, while others may map into a cusp on the symmetry plane of the corresponding group velocity surface. In these cases, Eqs. (11)–(15) for the QT mode are no longer valid.

The Young's modulus E_1 obtained in a tension test performed in the x_1 direction can be calculated using the elastic constants listed in Table 2 for three PEEK specimens. Denoting the elastic compliance matrix of a specimen with orthotropic symmetry by (S_{ij}), which is the inverse of the elastic stiffness matrix (C_{ij}), E_1 is expressed as

$$E_1 = 1/S_{11} = C_{11} - \frac{C_{33}C_{12} - C_{13}C_{23}}{C_{22}C_{33} - C_{13}C_{23}^2} C_{12} - \frac{C_{22}C_{13} - C_{12}C_{23}}{C_{22}C_{33} - C_{23}^2} C_{13}. \quad (16)$$

Using Eq. (16) and Table 2, one obtains for the Young's moduli E_1 of NT, GF, and CF PEEK specimens: 4.11 GPa, 10.8 GPa, and 24.0 GPa, respectively. The corresponding Young's moduli obtained from static tension tests performed in the x_1 direction and cited by the manufacturer of the specimens are 3.5 GPa, 8.4 GPa, and 23.0 GPa. The agreement is good for the CF PEEK specimen, and fair for the NT and GF PEEK specimens.

As mentioned earlier, the measured longitudinal moduli have a typical variation of several percent about their average, due largely to the inhomogeneity of materials, while the observed shear moduli have a typical variation of 10% about their average value. The latter variation is a combined effect of inhomogeneity of materials and a finite aperture of the source to the detector, both of which show apperature effects in the near field of relatively thin specimens. This latter effect becomes magnified in the measured mixed index elastic moduli that have a variation as large as 20% from the average values. As can be seen in Eqs. (14) and (15), small variations in V_g of the QL mode and the pure index elastic moduli resulting from material inhomogeneity and a small error in the source-to-detector angle ζ result in a large variation in the value of the mixed index elastic constant. These effects may partly explain the difference between the values of static and dynamic Young's moduli as observed above. The elastic constant data are also expected to vary appreciably from specimen

to specimen. The thermoelastic effect of the ultrasonically measured adiabatic Young's modulus and the dispersive effect of materials, which are beyond the scope of this investigation, will also give rise to the differences between the static and dynamic elastic moduli.

Detailed information on the use of both QL and QT group velocities within and without a cuspidal region for determination of elastic constants is found in Refs. 8 and 14.

Conclusion

In this work, we have demonstrated a novel method of determining all the elastic constants of orthotropic GF and CF PEEK specimens of relatively thin-plate shape from group velocity data measured in the symmetry planes by an essentially point-source/point-detector technique. The method is nondestructive without the need to cut or section the specimen in order to prepare additional parallel surfaces, which other conventional techniques may require for a similar purpose. Group velocities of the bulk QL and PT as well as a surface-skimming pseudo-L waves are used to determine all nine elastic constants.

Acknowledgement. K.Y. Kim and W. Sachse deeply appreciate the financial support of the Office of Naval Research (Solid Mechanics Program). A.R. Baker acknowledges the support of the Materials Science Center at Cornell University, which is funded by the National Science Foundation.

References

1. M.J.P. Musgrave. *Crystal Acoustics*. Holden-Day, San Francisco (1970)
2. B.A. Auld. *Acoustic Fields and Waves in Solids*, 2nd ed. Krieger, Malabar, FL (1990)
3. A.G. Every. *Phys. Rev.* **B22**:1746–1760 (1980)
4. H.J. McSkimin. In *Physical Acoustics*, edited by W.P. Mason. Vol. I, Part A, pp. 271–334. Academic Press, NY (1967)
5. E. Schreiber, O.L. Anderson, and M. Soga. *Elastic Constants and Their Measurements*. Academic Press, NY (1973)
6. E.P. Papadakis. In *Physical Acoustics*, edited by W.P. Mason and R.N. Thurston. Vol. XII, pp. 277–374. Academic Press, NY (1976)
7. S.I. Rokhlin and W. Wang. *J. Acoust. Soc. Am.* **91**:3303–3312 (1992)
8. K.Y. Kim. *Phys. Rev.* **B49**:3713–3724 (1994)
9. G.A. Northrop and J.P. Wolfe. In *Nonequilibrium Phonon Dynamics*, edited by W.E. Bron, pp. 165–242. Plenum Press, NY (1985)
10. A.G. Every. *Phys. Rev.* **B34**:2852–2862 (1986)
11. R.G. Payton. *Elastic Wave Propagation in Transversely Isotropic Media*. The Hague, Martinus Nijhoff (1983)
12. A.G. Every and K.Y. Kim. *J. Acoust. Soc. Am* **95**:2505–2516 (1994)
13. K.Y. Kim and W. Sachse. *J. Appl. Phys.* **75**:1435–1441 (1994)
14. K.Y. Kim, R. Sribar, and W. Sachse. *J. Appl. Phys.* **77**:5589–5600 (1995)
15. F.R. Breckenridge, C.E. Tschiegg, and M. Greenspan. *J. Acoust. Soc. Am.* **57**:626–631 (1975)
16. G.F.D. Duff. *Philos. Trans. R. Soc. London* **A252**:249–273 (1960)